1996AJ....112.2391H

THE ABSOLUTE LUMINOSITIES OF THE CALAN/TOLOLO TYPE Ia SUPERNOVAE

MARIO HAMUY,[1] M. M. PHILLIPS, ROBERT A. SCHOMMER, AND NICHOLAS B. SUNTZEFF

National Optical Astronomy Observatories,[2] Cerro Tololo Inter-American Observatory, Casilla 603, La Serena, Chile
Electronic mail: mhamuy@as.arizona.edu, mphillips@noao.edu, rschommer@noao.edu, nsuntzeff@noao.edu

JOSÉ MAZA[3]

Departamento de Astronomía, Universidad de Chile, Casilla 36-D, Santiago, Chile
Electronic mail: jmaza@das.uchile.cl

R. AVILÉS

National Optical Astronomy Observatories, Cerro Tololo Inter-American Observatory, Casilla 603, La Serena, Chile
Received 1996 January 10; revised 1996 September 5

ABSTRACT

We examine the absolute luminosities of 29 SNe Ia in the Calán/Tololo survey. We confirm a relation between the peak luminosity of the SNe and the decline rate as measured by the light curve, as suggested by Phillips [ApJ, 413, L105 (1993)]. We derive linear slopes to this magnitude-decline rate relation in $BV(I)_{KC}$ colors, using a sample with $B_{MAX} - V_{MAX} < 0.2^m$. The scatter around this linear relation (and thus the ability to measure SNe Ia distances) ranges from 0.13^m (in the I band) to 0.17^m (in the B band). We also find evidence for significant correlations between the absolute magnitudes or the decline rate of the light curve, and the morphological type of the host galaxy. © 1996 American Astronomical Society.

1. INTRODUCTION

Given the high intrinsic luminosities of type Ia supernovae (SNe Ia hereafter), considerable effort has been devoted during recent years to evaluating the usefulness of these objects as extragalactic distance indicators. Modern, high-quality photometry obtained with CCD detectors has revealed that SNe Ia display a wide range (>1 mag) of intrinsic optical luminosities at maximum light (e.g., Phillips 1993; Hamuy et al. 1995, hereafter referred to as Paper IV), potentially complicating the use of these objects as standard candles. There is also mounting evidence that the light curves of SNe Ia vary significantly in their shapes, and that these variations are correlated with the intrinsic brightness at maximum light (Phillips et al. 1987; Maza et al. 1994, hereafter Paper II; Paper IV; Suntzeff 1996).

More than 20 years ago, Barbon et al. (1973) suggested that SNe Ia could be divided into "fast" and "slow" decliners, depending on the initial decline rate of the B light curve. Pskovskii (1977, 1984) took this idea a step further, suggesting that the initial decline rates of SNe Ia were correlated with their intrinsic luminosities, with slow decliners being intrinsically brighter than fast decliners. Unfortunately, these results remained uncertain due to the relatively poor quality of the (mostly photographic) photometry available at that time and the related problem of contamination of these mea-

surements by the underlying light of the host galaxies (see Boisseau & Wheeler 1991). In addition, the samples of Barbon et al. and Pskovskii both included SNe which we now recognize to be type Ib/Ic events. Thus, the existence of a peak luminosity-decline rate relationship was widely doubted until three years ago, when Phillips (1993) reexamined the issue using a subsample of nine nearby, well-observed SNe Ia. With surface brightness fluctuations (SBF) and Tully–Fisher (T–F) distances available for these SNe, Phillips showed that the initial decline rate of the B light curve was, in fact, tightly correlated with the intrinsic B, V, and I maximum luminosity. This finding has significant implications for the use of this class of objects as extragalactic distance indicators since the initial decline rate could, in principle, be used to correct the apparent peak luminosity (in analogy to the period-luminosity relationship for Cepheid variables).

The Calán/Tololo SN survey, which was initiated at CTIO with the aim of discovering distant SNe (Hamuy et al. 1993a, hereafter referred to as Paper I), yielded 32 new SNe Ia in the redshift range $0.01 \leq z \leq 0.1$ during the period 1990–1993. Through the collaboration of many visiting astronomers, high-quality CCD light curves were obtained for nearly all of these discoveries. These SNe provide an independent opportunity to test the reality of the decline rate/intrinsic brightness relationship since they are at sufficiently large redshifts that the radial velocities of their host galaxies serve as an accurate indicator of their relative distances—and, hence, their relative luminosities. A preliminary study in the B and V bands was reported in Paper IV for 13 Calán/Tololo SNe Ia which confirmed in general terms the results

TABLE 1. Colors and absolute magnitudes of the Calán/Tololo supernovae Ia.

(1)	(2)	(3)	(4)	(5)	(6)	(7)	(8)
SN	$B_{MAX}-V_{MAX}$	M_{MAX}^B $+5\log(H_0/65)$	M_{MAX}^V $+5\log(H_0/65)$	M_{MAX}^I $+5\log(H_0/65)$	$\Delta m_{15}(B)$	$(B-V)_{gal}$ ± 0.10	Galaxy Type
90O	0.01(05)	-19.40(17)	-19.41(16)	-19.02(17)	0.96(10)	0.98	SBa
90T	0.04(10)	-19.17(24)	-19.21(19)	-18.98(19)	1.15(10)	0.71	Sa
90Y	0.33(10)	-18.56(24)	-18.89(20)	-18.65(19)	1.13(10)	0.56	E?
90af	0.05(03)	-18.95(11)	-19.00(11)	—	1.56(05)	0.92	SB0
91S	0.04(10)	-19.24(22)	-19.28(18)	-18.98(17)	1.04(10)	0.69	Sb
91U	0.06(10)	-19.49(25)	-19.55(21)	-19.37(20)	1.06(10)	0.71	Sbc
91ag	0.08(05)	-19.40(35)	-19.48(35)	-19.16(37)	0.87(10)	0.46	SBb
92J	0.12(10)	-18.92(23)	-19.04(19)	-18.78(18)	1.56(10)	0.95	E/S0
92K	0.74(10)	-17.72(44)	-18.46(42)	-18.61(42)	1.93(10)	0.86	SBb
92P	-0.03(03)	-19.34(18)	-19.31(18)	-19.03(18)	0.87(10)	0.73	SBa
92ae	0.11(05)	-19.07(13)	-19.18(10)	—	1.28(10)	0.53	E1?
92ag	0.13(05)	-18.98(19)	-19.11(18)	-18.98(18)	1.19(10)	0.68	S
92al	-0.05(03)	-19.47(32)	-19.42(31)	-19.13(31)	1.11(05)	0.60	Sb
92aq	0.10(05)	-18.89(10)	-18.99(08)	-18.57(10)	1.46(10)	1.02	Sa?
92au	0.05(10)	-19.03(22)	-19.08(18)	-18.83(17)	1.49(10)	0.87	E1
92bc	-0.08(03)	-19.64(23)	-19.56(23)	-19.22(22)	0.87(05)	0.66	Sab
92bg	-0.04(05)	-19.36(15)	-19.32(14)	-19.04(14)	1.15(10)	0.65	Sa
92bh	0.08(05)	-18.89(13)	-18.97(11)	-18.79(11)	1.05(10)	0.50	Sbc
92bk	0.00(05)	-19.03(12)	-19.03(10)	-18.83(10)	1.57(10)	0.96	E1
92bl	0.00(05)	-19.13(13)	-19.13(12)	-18.85(12)	1.51(10)	0.86	SB0/SBa
92bo	0.01(03)	-18.76(25)	-18.77(25)	-18.65(24)	1.69(05)	0.97	E5/S0
92bp	-0.05(05)	-19.40(09)	-19.35(08)	-19.03(08)	1.32(10)	0.72	E2/S0
92br	0.04(05)	-18.66(18)	-18.70(11)	—	1.69(10)	0.97	E0
92bs	0.07(05)	-18.96(11)	-19.03(10)	—	1.13(10)	0.51	SBb
93B	0.12(05)	-19.04(13)	-19.16(11)	-18.87(12)	1.04(10)	0.53	SBb
93H	0.23(05)	-18.45(19)	-18.68(19)	-18.74(19)	1.69(10)	0.84	SBb(rs)
93O	-0.09(03)	-19.23(11)	-19.14(10)	-18.91(10)	1.22(05)	0.66	E5/S01
93ag	0.03(05)	-19.10(12)	-19.13(11)	-18.81(11)	1.32(10)	0.80	E3/S01
93ah	-0.04(10)	-19.28(26)	-19.24(22)	-18.93(21)	1.30(10)	0.83	S02

of Phillips, although the slope of the relationship was less steep. With the entire Calán/Tololo database now reduced, a new analysis of this relationship seems in order. In this paper we report our definitive results based on light curves in the B, V, and I bands for the 27 best-observed Calán/Tololo events plus two additional distance SNe Ia for which similar data were obtained in our program. After a brief description of our sample (Sec. 2), we present in Sec. 3 a final version of the absolute magnitude vs. initial decline rate diagram for the Calán/Tololo events. This is compared in the same section with the luminosity-decline rate relation observed for an updated sample of nearby SNe Ia with SBF, Planetary Nebula Luminosity Function (PNLF), and Cepheid distances. Finally, in Sec. 4, both of these samples are used to reexamine the possibility (suggested in Paper IV) that the most luminous SNe Ia occur preferentially in galaxies having younger stellar populations. In accompanying papers, we present and discuss the Hubble diagram for the full set of Calán/Tololo SNe Ia (Hamuy *et al.* 1996a, hereafter Paper VI) and publish the individual $BV(I)_{KC}$ light curves (Hamuy *et al.* 1996b, hereafter Paper VII).

2. THE SAMPLES

2.1 Distant Sample

Of the 32 SNe Ia discovered during the course of the Calán/Tololo survey, adequately sampled $BV(I)_{KC}$ light curves were obtained for a total of 27 events. To this sample we have added two SNe Ia—1990O and 1992al—which, al-

though not found by us, were included in our program of followup photometry. Hence, the total sample of distant SNe Ia considered in this paper is 29.

Maximum-light magnitudes were measured directly from the observations whenever possible. We were able to perform this measurement for 11 SNe for which the time of the first photometric observation was no later than day+1 (counted since the peak of the B light curve), by fitting a low-order (3–4) polynomial to the data around maximum light. Among these 11 SNe, five of them possess well sampled light curves starting even a few days before peak and spanning through day +15, allowing thus a direct measurement of the initial decline rate of the B light curve. We performed this measurement by fitting higher-order (5–6) polynomials to the data gathered during the rising branch and the initial decline phase. For the majority of the events whose light curves were not sufficiently well sampled, or for which the follow-up observations did not begin until after maximum light, the peak magnitudes and initial decline rates were estimated using a χ^2-minimizing fitting procedure similar to that described in Paper IV. Note, however, that in order to include the I-band data, an updated and expanded set of $BV(I)_{KC}$ light curve templates were employed. This new set of templates are the subject of Paper VIII in this series Hamuy *et al.* 1996c). Further details of this fitting procedure are given in Paper VII.

Table 1 lists the 29 SNe and the relevant information for this study in the following format:

Column (1): SN name.

TABLE 2. Nearby SNe sample.

(1)	(2)	(3)	(4)	(5)	(6)	(7)	(8)	(9)	(10)	(11)	(12)
SN	Host Galaxy	Morph. Type	Distance Modulus	Distance Modulus References[a]	Method	Δm_{15}	E(B-V)	M^B_{MAX}	M^V_{MAX}	M^I_{MAX}	Photometry References[b]
37C	IC 4182	S/Irr	28.36(09)	1	Cepheids	0.87(10)	0.00(02)	-19.56(15)	-19.54(16)		1
72E	NGC 5253	Irr	27.97(07)	2	Cepheids	0.87(10)	0.05(02)	-19.69(18)	-19.64(18)	-19.26(21)	2
80N	NGC 1316	Sa$_{pec}$	31.23(06)	3,4	SBF/PNLF	1.28(04)	0.00(02)	-18.74(11)	-18.79(09)	-18.53(08)	3
81B	NGC 4536	Sc	31.10(13)	5	Cepheids	1.10(05)	0.00(02)	-19.07(16)	-19.17(15)		4,5,6
86G	NGC 5128	SO+S$_{pec}$	27.86(05)	3,4	SBF/PNLF	1.73(07)	0.65(10)	-18.08(42)	-18.43(32)	-18.45(22)	7
90N	NGC 4639	Sb	32.00(23)	6	Cepheids	1.07(05)	0.00(02)	-19.26(25)	-19.28(24)	-19.05(24)	8
91bg	NGC 4374	E1	31.26(05)	3	SBF	1.93(10)	0.03(02)	-16.62(14)	-17.38(09)	-17.81(08)	9,10
92A	NGC 1380	SO/Sa	31.00(10)	3	SBF	1.47(05)	0.00(02)	-18.43(13)	-18.45(12)	-18.20(11)	11
94D	NGC 4526	SO	30.86(08)	3	SBF	1.32(05)	0.00(02)	-19.00(12)	-18.96(11)	-18.75(09)	12

[a] References.- [1]Saha *et al.* (1994); [2]Saha *et al.* (1995); [3]Tonry (1996); [4]Ciardullo *et al.* (1993); [5]Saha *et al.* (1996); [6]Sandage *et al.* (1996).

[b] References.- [1]Pierce & Jacoby (1995); [2]Phillips & Eggen (1996); [3]Hamuy *et al.* (1991); [4]Buta & Turner (1983); [5]Barbon *et al.* (1982); [6]Tsvetkov (1982); [7]Phillips *et al.* (1987); [8]Lira (1995); [9]Filippenko *et al.* (1992); [10]Leibundgut *et al.* (1993); [11]Suntzeff *et al.* (1996); [12]Smith *et al.* (1996).

Column (2): the "color" of the SN, $B_{MAX} - V_{MAX}$.

Columns (3), (4), and (5): the absolute B, V, and I peak magnitudes of the SN calculated from the apparent magnitude, the redshift of the host galaxy (in the CMB frame), and an assumed Hubble constant $H_0 = 65$ km s^{-1} Mpc^{-1}. As we show in Paper VI, this value closely corresponds to the Hubble diagram of the distant SNe Ia with its zero point duly calibrated with Cepheid distances to nearby SNe Ia. These magnitudes were corrected for foreground extinction in the direction of the host galaxy (Burstein & Heiles 1982), and for the K terms calculated by Hamuy *et al.* (1993b). *Note however, that no correction has been applied for possible obscuration in the host galaxy (see Sec. 3).*

Column (6): the decline rate parameter $\Delta m_{15}(B)$, defined by Phillips (1993) as the amount in magnitudes that the B light curve decays in the first 15 days after maximum light. In most cases (24 SNe) this parameter was estimated through the template fitting procedure previously described in Hamuy *et al.* 1994 (hereafter referred to as Paper III) and Paper IV.

Column (7): the $B - V$ color of the host galaxy.

Column (8): the morphological type of the host galaxy following the classification scheme in The Hubble Atlas of Galaxies (Sandage 1961).

2.2 Nearby Sample

The sample of nearby SNe Ia employed in this paper is similar as that used by Phillips (1993), and consists of those events with (1) precise CCD or photoelectric photometry, (2) well-sampled light curves with coverage beginning either before or at maximum light, and (3) accurate relative distances measured for the host galaxy. The major difference with Phillips (1993) is that we have used only distances measured via Cepheids or the SBF and PNLF methods since there is growing evidence that the latter two techniques are on the same zero point as the Cepheids (Tonry 1996; Jacoby 1996).

Data for this revised sample are listed in Table 2. Note that, in several cases, the absolute magnitudes and decline rates in this table have changed somewhat with respect to those given by Phillips (1993). This is due either to the new distance moduli used (see above), the availability of improved photometry (SNe 1990N and 1992A), and/or slightly different assumptions of the dust extinction due to the host

galaxy (SN 1986G). The latter issue is discussed in more detail in Sec. 3. The format of Table 2 is as follows:

Column (1): SN name.

Column (2): the host galaxy.

Column (3): the host galaxy morphology following the classification scheme in The Hubble Atlas of Galaxies (Sandage 1961).

Column (4): the distance modulus of the host galaxy.

Column (5): references to the distance modulus given in column (4).

Column (6): the method used to determine the distance modulus (SBF=surface brightness fluctuations, PNLF =Planetary Nebulae luminosity function).

Column (7): the decline rate parameter $\Delta m_{15}(B)$ measured directly from the B light curve observations.

Column (8): the color excess E($B - V$). Except for SN 1986G, dust extinction due to the host galaxy has been ignored, and the quoted color excess are the Burstein & Heiles (1984) values for interstellar dust in our own galaxy. With this approach we wish to make the nearby sample reflect the properties of the distant sample for which we have not attempted to correct for possible obscuration in the host galaxies. For the highly reddened SN 1986G, we have estimated the reddening from the $B - V$ color evolution at late epochs (Lira 1995). Unfortunately, we are not able to apply this technique for the remaining SNe since the precision [$\pm 0.1^m$ in E($B - V$)] is not accurate enough to determine small reddenings.

Columns (9), (10), and (11): the absolute B, V, and I peak magnitudes of the SN calculated from the apparent magnitude, the distance modulus of the host galaxy, and the assumed color excess. A standard Galactic reddening law was assumed to convert the color excess to the extinction in the B, V, and I bands. In the case of SN 1986G, this may not be a good assumption (see Hough *et al.* 1987).

Column (12): references to the SN photometry. For SN 1994D we have preferred to use Smith *et al.* (1996) data instead of Richmond *et al.* (1995) because the former are on our own instrumental system. In any case, the differences between the two datasets are not greater than 0.05^m.
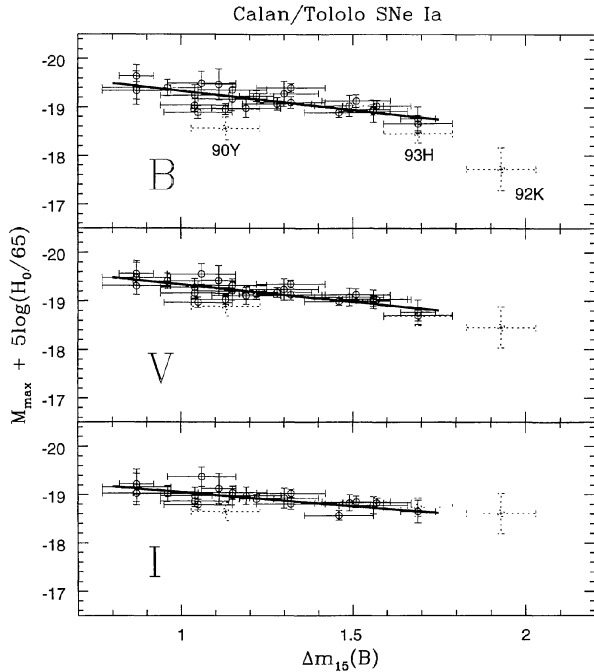
Calan/Tololo SNe Ia

FIG. 1. The absolute B, V, and I magnitudes (from Table 1) of the 29 Calán/Tololo SNe Ia plotted as a function of $\Delta m_{15}(B)$. Points with dotted error bars correspond to the two SNe (90Y and 93H) suspected to be significantly reddened by dust and to the intrinsically red SN 1992K. The ridge lines correspond to weighted linear least-squares fits to the remaining 26 (B & V) and 22 (I) SNe with $0.87 \leq \Delta m_{15}(B) \leq 1.69$.

3. PEAK LUMINOSITY-DECLINE RATE RELATION

Figure 1 shows the absolute magnitudes of the full sample of 29 distant SNe Ia plotted as a function of the decline rate parameter $\Delta m_{15}(B)$. The most obvious feature of this plot is the significant range in intrinsic luminosities displayed by the Calán/Tololo SNe, amounting to $\sim 2^m$ in B, $\sim 1^m$ in V, and $\sim 0\overset{m}{.}8$ in I. In general terms, these plots confirm the results of Phillips (1993) in the sense that SNe with slower decline rates tend to be intrinsically brighter than fast decliners. The scatter is clearly greatest in B, and decreases significantly in the V and I bands, as might be expected since we have not attempted to correct for possible dust extinction in the host galaxies. Ignoring SN 1992K, which is an intrinsically red object similar to the subluminous SN Ia 1991bg (Paper III), Table 1 shows that there are only two SNe in the sample with $B_{MAX} - V_{MAX} > 0.20$: 1990Y (0.33 ± 0.10) and 1993H (0.23 ± 0.05). In the case of SN 1993H, narrow Na I D absorption lines due to interstellar gas in the host galaxy were observed in the spectrum (equivalent width ~ 1.2 Å), suggesting that the red color at maximum light is, indeed, at least partially the product of uncorrected dust extinction. The case of SN 1990Y is less clear since the spectrum obtained by Filippenko & Shields (1990), which is the only one available to us, is of such low signal-to-noise that we can only place an uninteresting upper limit of 4 Å on the equivalent width of any possible interstellar Na I D absorption due to the host galaxy. For the remainder of this paper, we shall assume that the red color of this SN is also due to uncor-

TABLE 3. Least-squares fits. $M_{MAX} = a + b[\Delta m_{15}(B) - 1.1]$.

Bandpass	a	b	$\sigma(mag)$	χ^2_ν	n	sample
B	-19.258(0.048)	0.784(0.182)	0.17	1.24	26	"low extinction"
	-19.256(0.053)	0.860(0.210)	0.20	1.71	18	peak subsample
V	-19.267(0.042)	0.707(0.150)	0.14	0.97	26	"low extinction"
	-19.254(0.046)	0.743(0.173)	0.15	1.27	18	peak subsample
I	-18.993(0.044)	0.575(0.178)	0.13	0.85	22	"low extinction"
	-18.975(0.049)	0.654(0.231)	0.13	1.02	14	peak subsample

rected dust extinction (since this is the most likely explanation), but this cannot be proven beyond all doubt with the data at hand.

With the three red SNe excluded (1990Y, 1992K, and 1993H), the resulting range of colors of the Calán/Tololo SNe becomes significantly narrower (from -0.09 to $+0.13$). This leaves little room for large amounts of extinction in the parent galaxies and we also believe that, to some extent, some of the scatter in color is intrinsic (e.g., SNe 1992bc and 1992bo; Paper II). Note that a color cutoff (at $B - V > 0.25$) as an objective criteria to exclude contaminated objects was already proposed by Vaughan *et al.* (1995).

For the sake of simplicity, we have fitted straight lines to the data of Fig. 1. We have carried out weighted, linear, least-squares fits (Press *et al.* 1992) to the 26 remaining low-extinction Calán/Tololo SNe, shown as solid lines in Fig. 1. The parameters resulting from the fits to this subsample are summarized in Table 3. In addition we have tested a cut based on the completeness of the light-curve coverage at early times. Since $\Delta m_{15}(B)$ is a measurement of the decline rate over a short time interval after peak luminosity, we choose to exclude all SNe with no photometric measures within the first 5 days after the peak, thus eliminating 8 additional SNe (90T, 91S, 91U, 91ag, 92J, 92au, 92bk, and 93ah). The parameters derived in this restricted set of SNe (the second solution in Table 3) are insignificantly different (less than 1σ change) from those for the larger sample, and the reduced chi-squared (χ^2_ν) values and dispersion around the relation are not improved, so a restriction to this subsample does not appear to be necessary. Thus the preferred slopes are 0.784 ± 0.182 in B, 0.707 ± 0.150 in V, and 0.575 ± 0.178 in I.

The results presented above are essentially identical to our preliminary solutions obtained from a subsample of 11 SNe with a similar color cutoff (equations 11 and 12 of Paper IV), namely, 0.847 ± 0.128 in B and 0.787 ± 0.109 in V. The inclusion of the remaining Calán/Tololo SNe has significantly populated the absolute magnitude/decline rate diagram in the range $0.8 < \Delta m_{15}(B) < 1.7$, strongly confirming the reality of the magnitude-decline rate relationship.

In Fig. 2 the nearby sample of SNe Ia is shown superimposed on the Calán/Tololo points (excluding the two possibly reddened SNe 90Y and 93H). The combined data set is generally consistent with the relations shown in Fig. 1 and Table 3. As discussed in Paper IV, the Calán/Tololo slopes are significantly smaller than Phillips' original values, but much of this change comes about by restricting the sample in color. As also noted by Phillips, the slope of the absolute magnitude/decline rate relationship becomes smaller toward longer wavelengths. The differences seen in Fig. 2 between
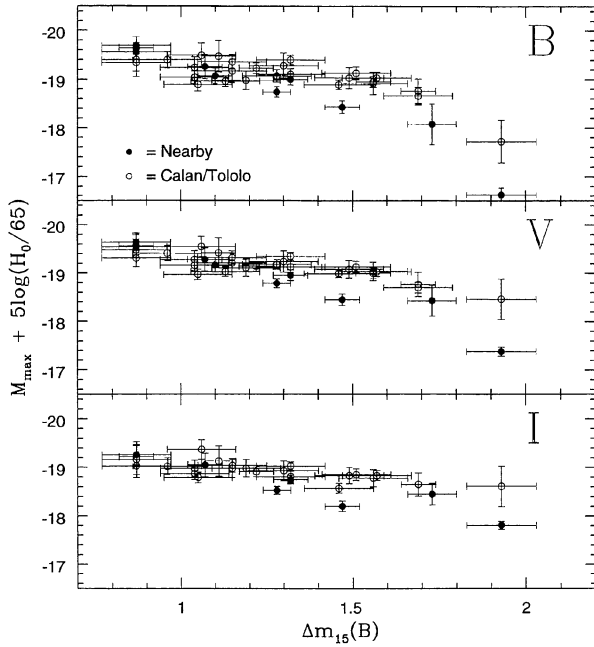
FIG. 2. As in Fig. 1, but with the open circles corresponding to the Calán/Tololo sample (excluding the two possibly reddened SNe 90Y and 93H), and the filled circles to the nearby sample (from Table 2).

the samples consist of two objects (SNe 92A and 91bg) being significantly fainter than the mean of the distant sample at the same $\Delta m_{15}(B)$. Based on the color criterion adopted above, SN 91bg would be excluded from the fits, but SN 92A would remain. While the photometry of the nearby sample is probably better than our distant sample, it is possible that the relative distances obtained from the Hubble law are more reliable than the SBF/PNLF distances used for the individual objects in the nearby sample, since the peculiar motions of the distant galaxies are a small fraction of their redshifs. We note that the nearby SNe with $\Delta m_{15}(B) > 1.2$ have distance moduli derived exclusively from SBF/PNLF, whereas all of the events with $\Delta m_{15}(B) < 1.2$ have Cepheid-based distances. Hence, any systematic differences between the two techniques would lead to a different slope compared to that of the distant sample. On the other hand, the Calán/Tololo sample suffers from a range of biases, including Malmquist effects; SNe fainter than $M_{MAX}^{B} \simeq -18.1$ would not be seen in more than 1/2 the volume of the survey (and indeed the faint SN 92K is the lowest redshift object in the sample). Thus the true SNe Ia luminosity function remains to be determined and the small differences seen in Fig. 2 have several possible explanations, although their effect on the derivation of the Hubble constant is probably small (see Paper VI).

4. MORPHOLOGICAL DEPENDENCIES

In Paper IV we investigated the relation between the luminosities of the SNe and their environments, and noticed that the most luminous objects were hosted by spiral galaxies. In that paper we separated the galaxies in two basic categories, namely, spirals and nonspirals. Given the large
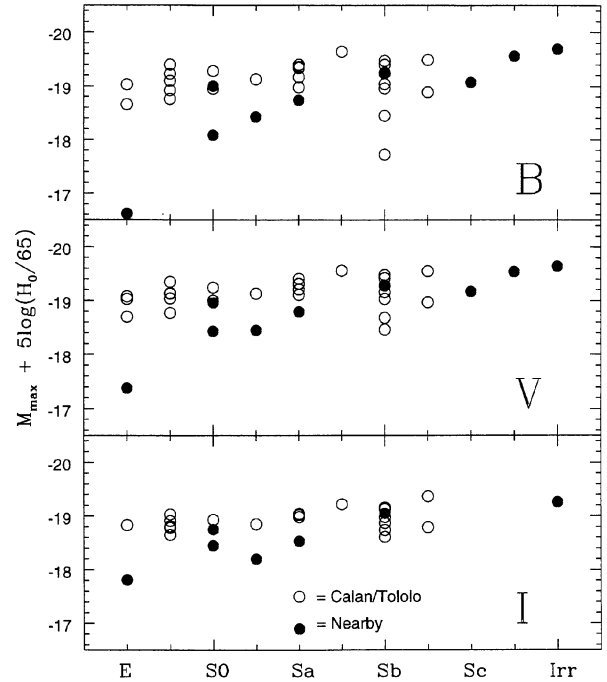

FIG. 3. The absolute B, V, and I magnitudes of the Calán/Tololo SNe Ia (open circles) and the nearby SNe (filled circles) plotted as a function of the morphological types of their host galaxies.

number of SNe included in this paper we have considered a finer grid of galaxy types, E, S0, Sa, Sb, Sc, and Irr. As can be seen in Table 1, in some cases the classification was intermediate between two categories, and in a few cases we were not able to provide an adequate classification (due to the distances of the galaxies). Figure 3 shows the absolute BVI magnitudes of the SNe listed in Table 1 and Table 2, plotted as a function of the morphological types of their parent galaxies. We recover our previous result in the sense that the brightest SNe occur in late-type galaxies, although admit-
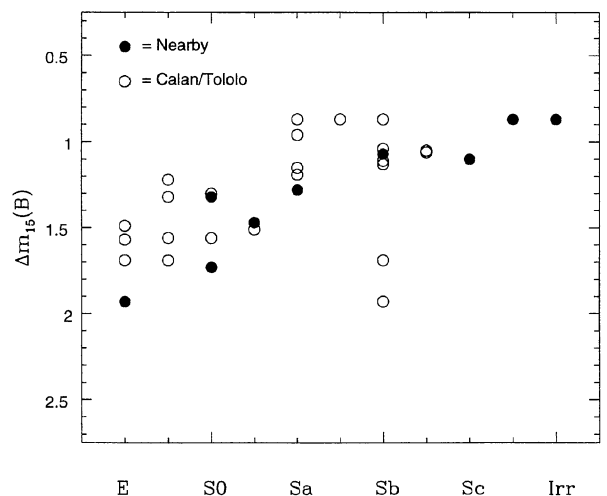

FIG. 4. The decline rate of the B light curve $[\Delta m_{15}(B)]$ of both the Calán/Tololo (open circles) and nearby (filled circles) samples of SNe Ia plotted as a function of the morphological types of their host galaxies.

tedly the effect is stronger in the nearby sample than in the Calán/Tololo SNe Ia. Note that this feature is not the result of uncorrected dust absorption, which would be expected to make SNe in spirals less luminous on average.

We find an even more striking relationship between the decline rate of the *B* light curves and the morphological classifications of the host galaxies. As shown in Fig. 4, SNe in spirals span a wide range in decline rates, whereas elliptical galaxies have not produced slow-decline SNe. Note that reddening has no effect on the points in this diagram. These results suggest that galaxies with a younger stellar population host the intrinsically brightest SNe Ia (slowest decliners). In this sense, the Calán/Tololo database provides a challenging opportunity to confront observations with a theory that can predict this morphological dependence of the SNe parameters.

5. DISCUSSION AND CONCLUSIONS

The application of the peak magnitude-decline rate relation permits a significantly reduced scatter in the SNe Ia Hubble diagram, to levels of 0.13^m–0.17^m. Without use of this relation, the mean magnitudes and dispersions for the Calán/Tololo sample (from Table 1) are: -19.05 ± 0.38 in *B*, -19.12 ± 0.26 in *V*, and -18.91 ± 0.20 in the *I* band. The reduction of σ by approximately a factor of 2 permits SNe Ia to be used as excellent distance indicators (with precisions in relative distances $\sim 7\%$–10%).

Recent work by Nugent *et al.* (1995) suggests that the correlation between peak luminosity and decline rate (Fig. 1) is related to a systematic variation in effective temperature, presumably corresponding to the amount of ^{56}Ni produced in the explosion. The origin of the relations between luminosity (Fig. 3) or decline rate (Fig. 4) and host galaxy morphological type are not understood at this point and need further theoretical exploration and modelling. The linear approximation to the luminosity-decline rate relation is all that is justified by the current data. Further study of the abnormal color SNe (e.g., SN 91bg and SN 92K) may provide clues to aspects of these relations.

A recent paper by Tammann & Sandage (1995; hereinafter T&S) calls into question the reality of the decline rate relation and any morphological dependences on SNe luminosity. The T&S version includes 10 SNe with "modern data" selected from Phillips (1993) and Paper IV, four SNe in Virgo cluster galaxies, and three other random SNe with $v > 1100$ km s^{-1} for which T&S provide their own estimates of the decline rate parameter $\Delta m_{15}(B)$. The 10 SNe with modern data show clear evidence for a correlation, which is not surprising since 7 of these are drawn from Paper IV. The four Virgo events show much more scatter, but this is also to be expected since no allowance has been made for the con-

siderable depth of the cluster. The three additional SNe (1970J, 1975N, 1976J) included in the diagram by T&S introduce further scatter but, again, this is not surprising since the data for these events is greatly inferior to that of the SNe with "modern data." Indeed, by including the latter 3 SNe (as well as 1984A from the Virgo subsample), T&S contradict their own statement that "the photometric data must be exquisite" to make a precise determination of $\Delta m_{15}(B)$.

From Fig. 2 of their paper, T&S conclude that the steepest allowable slopes for the decline rate-luminosity relation are 0.88 in *B* and 0.75 in *V*. Although their statement that these values are "factors of 3.1 and 2.6 smaller than the original Phillips (1993) result" is technically correct, it is important to realize that these steeper slopes were due largely to the inclusion of the low-luminosity event SN 1991bg which T&S specifically exclude from their sample on the grounds of spectroscopic peculiarity. Even more confusing, however, is T&S's statement that "the adopted slope values by Hamuy *et al.* of 1.62 in *B* and 1.76 in *V* are also larger than ours by an average factor of 2." In fact, Hamuy *et al.* give three different estimates for the slopes in *B* and *V*. The values quoted in T&S were derived from the six events in the Phillips (1993) nearby sample with $\Delta m_{15}(B) < 1.5$ and have large associated errors (1.624 ± 0.582 and 1.764 ± 0.570); the other estimates are 1.365 ± 0.275 in *B* and 1.142 ± 0.240 in *V* obtained with the Calán/Tololo SNe Ia with $\Delta m_{15}(B) < 1.5$, and 0.847 ± 0.128 in *B* and 0.787 ± 0.109 in *V* derived from the Calán/Tololo sample excluding only the 1991bg-like SN 1992K. The slopes derived by T&S should, of course, be compared with the latter values—not surprisingly (singe 7 of the 10 SNe in the T&S "modern data" sample are taken from Paper IV), they are very similar.

The new data presented in this paper both supports the reality of the decline rate–luminosity relation and strengthens the evidence for a dependence of the luminosity on the morphological type of the host galaxy. The conclusions of the T&S paper are based on confused comparisons with the results of our earlier papers and the addition of old, imprecise photographic data which dilutes and obscures the relations seen with higher-quality modern data.

REFERENCES

Barbon, R., Ciatti, F., & Rosino, L. 1973, A&A, 25, 241
Barbon, R., Ciatti, F., & Rosino, L. 1982, A&A, 116, 35
Boisseau, J. R., & Wheeler, J. C. 1991, AJ, 101, 1281
Burstein, D., & Heiles, C. 1982, AJ, 87, 1165

Burstein, D., & Heiles, C. 1984, ApJS, 54, 33
Buta, R. J., & Turner, A. 1983, PASP, 95, 72
Ciardullo, R. B., Jacoby, G. H., & Tonry, J. L. 1993, ApJ, 419, 479
Filippenko, A., & Shields, J. C. 1990, IAU Circ., No. 5083

Filippenko, A. V., *et al.* 1992, AJ, 104, 1543

Hamuy, M., Phillips, M. M., Maza, J., Wischnjewsky, M., Uomoto, A., Landolt, A. U., & Khatwani, R. 1991, AJ, 102, 208

Hamuy, M., *et al.* 1993a, AJ, 106, 2392 (Paper I)

Hamuy, M., Phillips, M. M., Wells, L. A., & Maza, J. 1993b, PASP, 105, 787

Hamuy, M., *et al.* 1994, AJ, 108, 2226 (Paper III)

Hamuy, M., Phillips, M. M., Maza, J., Suntzeff, N. B., Schommer, R. A., & Avilés, R. 1995, AJ, 109 1 (Paper IV)

Hamuy, M., Phillips, M. M., Suntzeff, N. B., Schommer, R. A., Maza, J., & Avilés, R. 1996a, AJ, 112, 2398 (Paper VI)

Hamuy, M., *et al.* 1996b, AJ, 112, 2408 (Paper VII)

Hamuy, M., Phillips, M. M., Suntzeff, N. B., Schommer, R. A., Maza, J., Smith, R. C., Lira, P., & Avilés, R. 1996c, AJ, 112, 2438 (Paper VIII)

Hough, J. H., Bailey, J. A., Rouse, M. F., & Whittet, C. B. 1987, MNRAS, 227, 1P

Jacoby, G. H. 1996, in Proceedings of The Extragalactic Distance Scale, STScI Spring meeting, edited by M. Livio, in preparation

Leibundgut, B., *et al.* 1993, AJ, 105, 301

Lira, P. 1995, MS thesis, Universidad de Chile

Maza, J., Hamuy, M., Phillips, M. M., Suntzeff, N. B., & Avilés, R. 1994, ApJ, 424, L107 (Paper II)

Nugent, P., Phillips, M., Baron, E., Branch, D., & Hauschildt, P. 1995, ApJ, 455, L147

Phillips, M. M., *et al.* 1987, PASP, 99, 592

Phillips, M. M. 1993, ApJ, 413, L105

Phillips, M. M., & Eggen, O. J. 1996, in preparation

Pierce, M. J., & Jacoby, G. H. 1995, AJ, 110, 2885

Press, W. H., Teukolsky, S. A., Vetterling, W. T., & Flannery, B. P. 1992, Numerical Recipes in Fortran, Second Edition (Cambridge University Press, Cambridge), pp. 660–664

Pskovskii, Y. P. 1977, SvA, 21, 675

Pskovskii, Y. P. 1984, SvA, 28, 658

Richmond, M. W., *et al.* 1995, AJ, 109, 2121

Saha, A., Labhardt, L., Schwengeler, H., Macchetto, F. D., Panagia, N., Sandage, A., & Tammann, G. A. 1994, ApJ, 425, 14

Saha, A., Sandage, A., Labhardt, L., Schwengeler, H., Tammann, G. A., Panagia, N., & Macchetto, F. D. 1995, ApJ, 438, 8

Saha, A., Sandage, A., Labhardt, L., Tammann, G. A., Macchetto, F. D., & Panagia, N. 1996, ApJ (in press)

Sandage, A. 1961, The Hubble Atlas of Galaxies (Carnegie Institution of Washington, Washington, DC)

Sandage, A., Saha, A., Tammann, G. A., Labhardt, L., Panagia, N., & Macchetto, F. D. 1996, ApJ, 460, L15

Smith, R. C., *et al.* 1996, in preparation

Suntzeff, N. B. 1996, in Supernovae and Supernova Remnants, IAU Colloquium 145, edited by R. McCray (Cambridge University Press, Cambridge) (in press)

Tammann, G. A., & Sandage, A. 1995, ApJ, 452, 16 (T&S)

Tonry, J. L. 1996, in Proceedings of The Extragalactic Distance Scale, STScI Spring meeting, edited by M. Livio, in preparation

Tsvetkov, D. Y. 1982, SvAL, 8, 115

Vaughan, T. E., Branch, D., Miller, D. L., & Perlmutter, S. 1995, ApJ, 439, 558